arXiv:1606.05126v1 [hep-ph] 16 Jun 2016

Exclusive diffractive production of $\pi^+\pi^-\pi^+\pi^-$ via the intermediate $\sigma\sigma$ and $\rho\rho$ states in proton-proton collisions within tensor pomeron approach

Piotr Lebiedowicz,[1,*] Otto Nachtmann,[2,†] and Antoni Szczurek [‡1,§]

[1] *Institute of Nuclear Physics PAN, PL-31-342 Kraków, Poland*
[2] *Institut für Theoretische Physik, Universität Heidelberg, Philosophenweg 16, D-69120 Heidelberg, Germany*

Abstract

We present first predictions of the cross sections and differential distributions for the central exclusive reaction $pp \to pp\pi^+\pi^-\pi^+\pi^-$ being studied at RHIC and LHC. The amplitudes for the processes are formulated in terms of the tensor pomeron and tensor $f_{2\mathbb{R}}$ reggeon exchanges with the vertices respecting the standard crossing and charge-conjugation relations of Quantum Field Theory. The $\sigma\sigma$ and $\rho\rho$ contributions to the $\pi^+\pi^-\pi^+\pi^-$ final state are considered focussing on their specificities. The correct inclusion of the pomeron spin structure seems crucial for the considered sequential mechanisms in particular for the $\rho\rho$ contribution which is treated here for the first time. The mechanism considered gives a significant contribution to the $pp \to pp\pi^+\pi^-\pi^+\pi^-$ reaction. We adjust parameters of our model to the CERN-ISR experimental data and present several predictions for the STAR, ALICE, ATLAS and CMS experiments. A measurable cross section of order of a few μb is obtained including the experimental cuts relevant for the LHC experiments. We show the influence of the experimental cuts on the integrated cross section and on various differential distributions.

PACS numbers: 12.40.Nn,13.60.Le,14.40.Be

‡ also at University of Rzeszów, PL-35-959 Rzeszów, Poland.
*Electronic address: Piotr.Lebiedowicz@ifj.edu.pl
†Electronic address: O.Nachtmann@thphys.uni-heidelberg.de
§Electronic address: Antoni.Szczurek@ifj.edu.pl

I. INTRODUCTION

Last years there was a renewed interest in exclusive production of two meson pairs (mostly $\pi^+\pi^-$ pairs) at high energies related to planned experiments at RHIC [1], Tevatron [2, 3], and LHC [4–6]. From the experimental point of view the exclusive processes are important in the context of resonance production, in particular, in searches for glueballs. The experimental data on central exclusive $\pi^+\pi^-$ production measured at the energies of the ISR, RHIC, Tevatron, and the LHC collider all show visible structures in the $\pi^+\pi^-$ invariant mass. It is found that the pattern of these structures seems to depend on experiment. But, as we advocated in Ref. [7], this dependence could be due to the cuts used in a particular experiment (usually these cuts are different for different experiments).

So far theoretical studies concentrated on two-pion continuum production. Some time ago two of us have formulated a Regge-type model with parameters fixed from phenomenological analysis of total and elastic NN and πN scattering [8]. The model was extended to include also absorption effects due to proton-proton interaction [9, 10]. In Ref. [9] the exclusive reaction $pp \to pp\pi^+\pi^-$ constitutes an irreducible background to the scalar χ_{c0} meson production. These model studies were extended also to K^+K^- production [10]. For a related work on the exclusive reaction $pp \to nn\pi^+\pi^+$, see [11]. A revised view of the absorption effects including the πN nonperturbative interactions was presented very recently [12]. Such an approach gives correct order of magnitude cross sections, however, does not include resonance contributions which interfere with the continuum.

It was known for a long time that the frequently used vector-pomeron model has problems considering a field theory point of view. Taken literally it gives opposite signs for pp and $\bar{p}p$ total cross sections. A way out of these problems was already shown in [13] where the pomeron was described as a coherent superposition of exchanges with spin 2 + 4 + 6 + ... The same idea is realised in the tensor-pomeron model formulated in [14]. In this model pomeron exchange can effectively be treated as the exchange of a rank-2 symmetric tensor. The corresponding couplings of the tensorial object to proton and pion were worked out. In Ref. [15] the model was applied to the diffractive production of several scalar and pseudoscalar mesons in the reaction $pp \to ppM$. In [16] an extensive study of the photoproduction reaction $\gamma p \to \pi^+\pi^- p$ in the framework of the tensor-pomeron model was presented. The resonant ($\rho^0 \to \pi^+\pi^-$) and non-resonant (Drell-Söding) photon-pomeron/reggeon $\pi^+\pi^-$ production in pp collisions was studied in [17]. The exclusive diffractive production of $\pi^+\pi^-$ continuum together with the dominant scalar $f_0(500)$, $f_0(980)$, and tensor $f_2(1270)$ resonances was studied by us very recently in Ref. [7].

The past program of central production of pairs of mesons was concentrated on the discussion of mesonic resonances. The low-energy program of studying meson excitations can be repeated at the LHC, where we expect dominance of one production mechanism only, two-pomeron exchange.

The identification of glueballs can be very difficult. The partial wave analyses of future experimental data of the STAR, ALICE, ATLAS and CMS Collaborations could be used in this context. Also the studies of different decay channels in central exclusive production would be very valuable. One of the possibilities is the $pp \to pp\pi^+\pi^-\pi^+\pi^-$ reaction being analysed by the ATLAS, CMS and ALICE Collaborations at the LHC. Identification

of the glueball-like states in this channel requires calculation/estimation of the four-pion background from other sources.

Pairs of $\rho^0\rho^0$ (giving four pions) can be produced also in photon-hadron interactions in a so-called double scattering mechanism. In Ref. [18] double vector meson production in photon-photon and photon-hadron interactions in $pp/pA/AA$ collisions was studied. In heavy ion collisions the double scattering mechanism is very important [18, 19]. In proton-proton collisions, for instance at the center-of-mass energy of $\sqrt{s} = 7$ TeV, total cross sections for the double ρ^0 meson production, taking into account the $\gamma\gamma$ and double scattering mechanisms, were estimated [18] to be of 182 pb and 4 pb, respectively.

In the present paper we wish to concentrate on the four charged pion continuum which is a background for future studies of diffractively produced resonances. We shall present a first evaluation of the four-pion continuum in the framework of the tensor pomeron model consistent with general rules of Quantum Field Theory. Here we shall give explicit expressions for the amplitudes of $\rho\rho \equiv \rho(770)\rho(770)$ and $\sigma\sigma \equiv f_0(500)f_0(500)$ production with the ρ and σ decaying to $\pi^+\pi^-$. We shall discuss their specificity and relevance for the $pp \to pp\pi^+\pi^-\pi^+\pi^-$ reaction. In the Appendix A we present the formulas of the double-pomeron exchange mechanism for the exclusive production of scalar resonances decaying into $\sigma\sigma$ and/or $\rho\rho$ pairs.

II. EXCLUSIVE DIFFRACTIVE PRODUCTION OF FOUR PIONS

In the present paper we consider the $2 \to 6$ processes from the diagrams shown in Fig. 1,

$$\begin{aligned} pp &\to pp\,\sigma\sigma \to pp\,\pi^+\pi^-\pi^+\pi^-\,, \\ pp &\to pp\,\rho\rho \to pp\,\pi^+\pi^-\pi^+\pi^-\,. \end{aligned} \tag{2.1}$$

That is, we treat effectively the $2 \to 6$ processes (2.1) as arising from $2 \to 4$ processes, the central diffractive production of two scalar σ mesons and two vector ρ mesons in proton-proton collisions. To calculate the total cross section for the $2 \to 4$ reactions one has to calculate the 8-dimensional phase-space integral numerically [8] [1]. Some modifications of the $2 \to 4$ reaction are needed to simulate the $2 \to 6$ reaction with $\pi^+\pi^-\pi^+\pi^-$ in the final state. For example, one has to include in addition a smearing of the σ and ρ masses due to their instabilities. Then, the general cross-section formula can be written approximately as

$$\sigma_{2\to6} = \int_{2m_\pi}^{\max\{m_{X_3}\}} \int_{2m_\pi}^{\max\{m_{X_4}\}} \sigma_{2\to4}(..., m_{X_3}, m_{X_4})\, f_M(m_{X_3})\, f_M(m_{X_4})\, dm_{X_3}\, dm_{X_4}\,. \tag{2.2}$$

Here we use for the calculation of the decay processes $M \to \pi^+\pi^-$ with $M = \sigma, \rho$ the spectral function

$$f_M(m_{X_i}) = \left(1 - \frac{4m_\pi^2}{m_{X_i}^2}\right)^{n/2} \frac{\frac{2}{\pi} m_M^2 \Gamma_{M,tot}}{(m_{X_i}^2 - m_M^2)^2 + m_M^2 \Gamma_{M,tot}^2}\, N_I\,, \tag{2.3}$$

[1] In the integration over four-body phase space the transverse momenta of the produced particles (p_{1t}, p_{2t}, p_{3t}, p_{4t}), the azimuthal angles of the outgoing protons (ϕ_1, ϕ_2) and the rapidity of the produced mesons (y_3, y_4) were chosen as integration variables over the phase space.

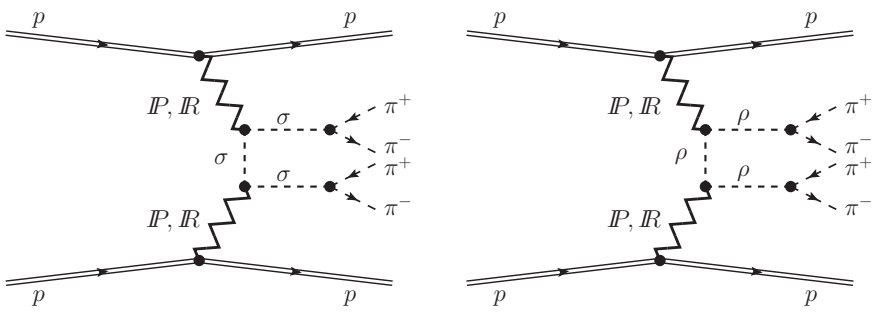

FIG. 1: The "Born level" diagrams for double-pomeron/reggeon central exclusive $\sigma\sigma$ (left diagram) and $\rho\rho$ (right diagram) production and their subsequent decays into $\pi^+\pi^-\pi^+\pi^-$ in proton-proton collisions.

where $i = 3, 4$. In (2.3) $n = 3$, $N_I = 1$ for ρ meson and $n = 1$, $N_I = \frac{2}{3}$ for σ meson, respectively. The quantity $\left(1 - 4m_\pi^2/m_{X_i}^2\right)^{n/2}$ smoothly decreases the spectral function when approaching the $\pi^+\pi^-$ threshold, $m_{X_i} \to 2m_\pi$.

A. $pp \to pp\sigma\sigma$

Here we discuss the exclusive production of $\sigma\sigma \equiv f_0(500)f_0(500)$ pairs in proton-proton collisions,

$$p(p_a, \lambda_a) + p(p_b, \lambda_b) \to p(p_1, \lambda_1) + \sigma(p_3) + \sigma(p_4) + p(p_2, \lambda_2)\,, \tag{2.4}$$

where $p_{a,b}$, $p_{1,2}$ and $\lambda_{a,b}$, $\lambda_{1,2} = \pm\frac{1}{2}$ denote the four-momenta and helicities of the protons and $p_{3,4}$ denote the four-momenta of the mesons, respectively.

The diagram for the $\sigma\sigma$ production with an intermediate σ meson is shown in Fig. 1 (left diagram). The amplitude for this process can be written as the following sum:

$$\mathcal{M}_{pp\to pp\sigma\sigma}^{(\sigma-\text{exchange})} = \mathcal{M}^{(\mathbb{P}\mathbb{P}\to\sigma\sigma)} + \mathcal{M}^{(\mathbb{P}f_{2\mathbb{R}}\to\sigma\sigma)} + \mathcal{M}^{(f_{2\mathbb{R}}\mathbb{P}\to\sigma\sigma)} + \mathcal{M}^{(f_{2\mathbb{R}}f_{2\mathbb{R}}\to\sigma\sigma)}\,. \tag{2.5}$$

For instance, the $\mathbb{P}\mathbb{P}$-exchange amplitude can be written as

$$\mathcal{M}^{(\mathbb{P}\mathbb{P}\to\sigma\sigma)} = \mathcal{M}^{(\hat{t})}_{\lambda_a\lambda_b\to\lambda_1\lambda_2\sigma\sigma} + \mathcal{M}^{(\hat{u})}_{\lambda_a\lambda_b\to\lambda_1\lambda_2\sigma\sigma} \tag{2.6}$$

with the $\hat{t}$- and $\hat{u}$-channel amplitudes

$$\begin{aligned}
&\mathcal{M}^{(\hat{t})}_{\lambda_a\lambda_b\to\lambda_1\lambda_2\sigma\sigma} = \\
&\quad (-i)\bar{u}(p_1,\lambda_1) i\Gamma^{(\mathbb{P}pp)}_{\mu_1\nu_1}(p_1,p_a) u(p_a,\lambda_a)\, i\Delta^{(\mathbb{P})\,\mu_1\nu_1,\alpha_1\beta_1}(s_{13},t_1)\, i\Gamma^{(\mathbb{P}\sigma\sigma)}_{\alpha_1\beta_1}(p_t,-p_3)\, i\Delta^{(\sigma)}(p_t) \\
&\quad \times i\Gamma^{(\mathbb{P}\sigma\sigma)}_{\alpha_2\beta_2}(p_4,p_t)\, i\Delta^{(\mathbb{P})\,\alpha_2\beta_2,\mu_2\nu_2}(s_{24},t_2)\, \bar{u}(p_2,\lambda_2) i\Gamma^{(\mathbb{P}pp)}_{\mu_2\nu_2}(p_2,p_b) u(p_b,\lambda_b)\,,
\end{aligned} \tag{2.7}$$

$$
\begin{aligned}
&\mathcal{M}^{(\hat{u})}_{\lambda_a\lambda_b\to\lambda_1\lambda_2\sigma\sigma} = \\
&\quad (-i)\,\bar{u}(p_1,\lambda_1) i\Gamma^{(\mathbb{P}pp)}_{\mu_1\nu_1}(p_1,p_a) u(p_a,\lambda_a)\, i\Delta^{(\mathbb{P})\,\mu_1\nu_1,\alpha_1\beta_1}(s_{14},t_1)\, i\Gamma^{(\mathbb{P}\sigma\sigma)}_{\alpha_1\beta_1}(p_4,p_u)\, i\Delta^{(\sigma)}(p_u) \\
&\quad \times i\Gamma^{(\mathbb{P}\sigma\sigma)}_{\alpha_2\beta_2}(p_u,-p_3)\, i\Delta^{(\mathbb{P})\,\alpha_2\beta_2,\mu_2\nu_2}(s_{23},t_2)\, \bar{u}(p_2,\lambda_2) i\Gamma^{(\mathbb{P}pp)}_{\mu_2\nu_2}(p_2,p_b) u(p_b,\lambda_b)\,,
\end{aligned}
\tag{2.8}
$$

where $p_t = p_a - p_1 - p_3$, $p_u = p_4 - p_a + p_1$, $s_{ij} = (p_i + p_j)^2$, $t_1 = (p_1 - p_a)^2$, $t_2 = (p_2 - p_b)^2$. Here $\Delta^{(\mathbb{P})}$ and $\Gamma^{(\mathbb{P}pp)}$ denote the effective propagator and proton vertex function, respectively, for the tensorial pomeron. The effective propagators and vertex functions for the tensorial pomeron/reggeon exchanges respect the standard crossing and charge-conjugation relations of Quantum Field Theory. For the explicit expressions of these terms see Sect. 3 of [14]. We assume that $\Gamma^{(\mathbb{P}\sigma\sigma)}$ has the same form as $\Gamma^{(\mathbb{P}\pi\pi)}$ (see (3.45) of [14]) but with the $\mathbb{P}\sigma\sigma$ coupling constant $g_{\mathbb{P}\sigma\sigma}$ instead of the $\mathbb{P}\pi\pi$ one $2\beta_{\mathbb{P}\pi\pi}$. The scalar meson propagator $\Delta^{(\sigma)}$ is taken as in (4.7) and (4.8) of [7] with the running (energy-dependent) width. In a similar way the $\mathbb{P}f_{2\mathbb{R}}$, $f_{2\mathbb{R}}\mathbb{P}$ and $f_{2\mathbb{R}}f_{2\mathbb{R}}$ amplitudes can be written. For the $f_{2\mathbb{R}}\sigma\sigma$ vertex our ansatz is as for $f_{2\mathbb{R}}\pi\pi$ in (3.53) of [14] but with $g_{f_{2\mathbb{R}}\pi\pi}$ replaced by $g_{f_{2\mathbb{R}}\sigma\sigma}$.

In the high-energy small-angle approximation we can write the $2\to 4$ amplitude (2.5) as

$$
\begin{aligned}
\mathcal{M}^{(\sigma-\text{exchange})}_{\lambda_a\lambda_b\to\lambda_1\lambda_2\sigma\sigma} \simeq\ & 2(p_1+p_a)_{\mu_1}(p_1+p_a)_{\nu_1}\,\delta_{\lambda_1\lambda_a}\,F_1(t_1)\,F_M(t_1) \\
&\times\Big\{ V^{\mu_1\nu_1}(s_{13},t_1,p_t,-p_3)\ \Delta^{(\sigma)}(p_t)\ V^{\mu_2\nu_2}(s_{24},t_2,p_t,p_4)\ \Big[\hat{F}_\sigma(p_t^2)\Big]^2 \\
&\quad + V^{\mu_1\nu_1}(s_{14},t_1,p_u,p_4)\ \Delta^{(\sigma)}(p_u)\ V^{\mu_2\nu_2}(s_{23},t_2,p_u,-p_3)\ \Big[\hat{F}_\sigma(p_u^2)\Big]^2 \Big\} \\
&\times 2(p_2+p_b)_{\mu_2}(p_2+p_b)_{\nu_2}\,\delta_{\lambda_2\lambda_b}\,F_1(t_2)\,F_M(t_2)\,.
\end{aligned}
\tag{2.9}
$$

The function $V_{\mu\nu}$ has the form ($M_0 \equiv 1$ GeV)

$$
\begin{aligned}
V_{\mu\nu}(s,t,k_2,k_1) =& (k_1+k_2)_\mu(k_1+k_2)_\nu\ \frac{1}{4s}\Big[3\beta_{\mathbb{P}NN}\, g_{\mathbb{P}\sigma\sigma}(-is\alpha'_{\mathbb{P}})^{\alpha_{\mathbb{P}}(t)-1} \\
&+ \frac{1}{2M_0^2} g_{f_{2\mathbb{R}}pp}\, g_{f_{2\mathbb{R}}\sigma\sigma}(-is\alpha'_{f_{2\mathbb{R}}})^{\alpha_{f_{2\mathbb{R}}}(t)-1}\Big]\,,
\end{aligned}
\tag{2.10}
$$

where $\beta_{\mathbb{P}NN} = 1.87\ \text{GeV}^{-1}$ and $g_{f_{2\mathbb{R}}pp} = 11.04$ from (6.53) and (6.55) of [14], respectively.

If the σ meson has substantial gluon content or some $q\bar{q}q\bar{q}$ component its coupling to $\mathbb{P}$ and $f_{2\mathbb{R}}$ may be larger than for the pion. To illustrate effects of this possibility we take in the calculation two sets of the coupling constants

$$
\text{set A}: \quad g_{\mathbb{P}\sigma\sigma} = 2\beta_{\mathbb{P}\pi\pi}\,, \quad g_{f_{2\mathbb{R}}\sigma\sigma} = g_{f_{2\mathbb{R}}\pi\pi}\,, \tag{2.11}
$$

$$
\text{set B}: \quad g_{\mathbb{P}\sigma\sigma} = 4\beta_{\mathbb{P}\pi\pi}\,, \quad g_{f_{2\mathbb{R}}\sigma\sigma} = 2g_{f_{2\mathbb{R}}\pi\pi}\,, \tag{2.12}
$$

where $\beta_{\mathbb{P}\pi\pi} = 1.76\ \text{GeV}^{-1}$ and $g_{f_{2\mathbb{R}}\pi\pi} = 9.30$ from (7.15) and (7.16) of [14], respectively.

The form of the off-shell meson form factor $\hat{F}_\sigma(k^2)$ in (2.9) and of the analogous form factor for ρ mesons $\hat{F}_\rho(k^2)$ (see the next section) is unknown. We write generically $\hat{F}_M(k^2)$

$(M = \sigma, \rho)$ for these form factors which we normalize to unity at the on-shell point, $\hat{F}_M(m_M^2) = 1$, and parametrise here in two ways:

$$\hat{F}_M(k^2) = \exp\left(\frac{k^2 - m_M^2}{\Lambda_{off,E}^2}\right), \tag{2.13}$$

$$\hat{F}_M(k^2) = \frac{\Lambda_{off,Mp}^2 - m_M^2}{\Lambda_{off,Mp}^2 - k^2}, \quad \Lambda_{off,Mp} > m_M. \tag{2.14}$$

The cut-off parameters $\Lambda_{off,E}$ for the exponential form or $\Lambda_{off,Mp}$ for the monopole form of the form factors can be adjusted to experimental data.

A factor $\frac{1}{2}$ due to the identity of the two σ mesons in the final state has to be taken into account in the phase-space integration in (2.2).

B. $pp \to pp\rho\rho$

Here we focus on exclusive production of $\rho\rho \equiv \rho(770)\rho(770)$ in proton-proton collisions, see Fig. 1 (right diagram),

$$p(p_a, \lambda_a) + p(p_b, \lambda_b) \to p(p_1, \lambda_1) + \rho(p_3, \lambda_3) + \rho(p_4, \lambda_4) + p(p_2, \lambda_2), \tag{2.15}$$

where $p_{3,4}$ and $\lambda_{3,4} = 0, \pm 1$ denote the four-momenta and helicities of the ρ mesons, respectively. We write the amplitude as

$$\mathcal{M}_{\lambda_a\lambda_b\to\lambda_1\lambda_2\rho\rho} = \left(\epsilon_{\rho_3}^{(\rho)}(\lambda_3)\right)^* \left(\epsilon_{\rho_4}^{(\rho)}(\lambda_4)\right)^* \mathcal{M}^{\rho_3\rho_4}_{\lambda_a\lambda_b\to\lambda_1\lambda_2\rho\rho}, \tag{2.16}$$

where $\epsilon_\rho^{(\rho)}(\lambda)$ are the polarisation vectors of the ρ meson.

Then, with the expressions for the propagators, vertices, and form factors, from [14] $\mathcal{M}^{\rho_3\rho_4}$ can be written in the high-energy approximation as

$$\begin{aligned}
&\mathcal{M}^{(\rho-\text{exchange})\,\rho_3\rho_4}_{\lambda_a\lambda_b\to\lambda_1\lambda_2\rho\rho} \simeq\; 2(p_1+p_a)_{\mu_1}(p_1+p_a)_{\nu_1}\,\delta_{\lambda_1\lambda_a}\,F_1(t_1)\,F_M(t_1) \\
&\times\Bigg\{ V^{\rho_3\rho_1\mu_1\nu_1}(s_{13}, t_1, p_t, p_3)\;\Delta^{(\rho)}_{\rho_1\rho_2}(p_t)\;V^{\rho_4\rho_2\mu_2\nu_2}(s_{24}, t_2, -p_t, p_4)\;\left[\hat{F}_\rho(p_t^2)\right]^2 \\
&\quad + V^{\rho_4\rho_1\mu_1\nu_1}(s_{14}, t_1, -p_u, p_4)\;\Delta^{(\rho)}_{\rho_1\rho_2}(p_u)\;V^{\rho_3\rho_2\mu_2\nu_2}(s_{23}, t_2, p_u, p_3)\;\left[\hat{F}_\rho(p_u^2)\right]^2 \Bigg\} \\
&\times 2(p_2+p_b)_{\mu_2}(p_2+p_b)_{\nu_2}\,\delta_{\lambda_2\lambda_b}\,F_1(t_2)\,F_M(t_2),
\end{aligned} \tag{2.17}$$

where $V_{\mu\nu\kappa\lambda}$ reads as

$$\begin{aligned}
V_{\mu\nu\kappa\lambda}(s,t,k_2,k_1) =& 2\Gamma^{(0)}_{\mu\nu\kappa\lambda}(k_1,k_2)\frac{1}{4s}\Bigg[3\beta_{\mathbb{P}NN}\,a_{\mathbb{P}\rho\rho}(-is\alpha'_{\mathbb{P}})^{\alpha_{\mathbb{P}}(t)-1} \\
&\qquad + \frac{1}{M_0}g_{f_{2\mathbb{R}}pp}\,a_{f_{2\mathbb{R}}\rho\rho}(-is\alpha'_{f_{2\mathbb{R}}})^{\alpha_{f_{2\mathbb{R}}}(t)-1}\Bigg] \\
&- \Gamma^{(2)}_{\mu\nu\kappa\lambda}(k_1,k_2)\frac{1}{4s}\Bigg[3\beta_{\mathbb{P}NN}\,b_{\mathbb{P}\rho\rho}(-is\alpha'_{\mathbb{P}})^{\alpha_{\mathbb{P}}(t)-1} \\
&\qquad + \frac{1}{M_0}g_{f_{2\mathbb{R}}pp}\,b_{f_{2\mathbb{R}}\rho\rho}(-is\alpha'_{f_{2\mathbb{R}}})^{\alpha_{f_{2\mathbb{R}}}(t)-1}\Bigg].
\end{aligned} \tag{2.18}$$

The explicit tensorial functions $\Gamma^{(i)}_{\mu\nu\kappa\lambda}(k_1, k_2)$, $i = 0, 2$, are given in Ref. [14], see formulae (3.18) and (3.19), respectively. In our calculations the parameter set A of coupling constants a and b from [17] was used, see Eq. (2.15) there.

We consider in (2.15) unpolarised protons in the initial state and no observation of polarizations in the final state. In the following we are mostly interested in the invariant mass distributions of the 4π system and in distributions of the parent ρ mesons. Therefore, we have to insert in (2.2) the cross section $\sigma_{2\to4}$ summed over the ρ meson polarizations. The spin sum for a ρ meson of momentum k and squared mass $k^2 = m_X^2$ is

$$\sum_{\lambda=0,\pm1} \epsilon^{(\rho)\,\mu}(\lambda) \left(\epsilon^{(\rho)\,\nu}(\lambda)\right)^* = -g^{\mu\nu} + \frac{k^\mu k^\nu}{m_X^2}\,. \tag{2.19}$$

But the $k^\mu k^\nu$ terms do not contribute since we have the relations

$$p_{3\,\rho_3} \mathcal{M}^{\rho_3\rho_4}_{\lambda_a\lambda_b\to\lambda_1\lambda_2\rho\rho} = 0\,, \qquad p_{4\,\rho_4} \mathcal{M}^{\rho_3\rho_4}_{\lambda_a\lambda_b\to\lambda_1\lambda_2\rho\rho} = 0\,. \tag{2.20}$$

These follow from the properties of $\Gamma^{(0,2)}_{\mu\nu\kappa\lambda}$ in (2.18); see (3.21) of [14].

Taking also into account the statistical factor $\frac{1}{2}$ due to the identity of the two ρ mesons we get for the amplitudes squared (to be inserted in $\sigma_{2\to4}$ in (2.2))

$$\begin{aligned} &\frac{1}{2}\frac{1}{4} \sum_{\text{spins}} \left| \left(\epsilon^{(\rho)}_{\rho_3}(\lambda_3)\right)^* \left(\epsilon^{(\rho)}_{\rho_4}(\lambda_4)\right)^* \mathcal{M}^{\rho_3\rho_4}_{\lambda_a\lambda_b\to\lambda_1\lambda_2\rho\rho} \right|^2 \\ &= \frac{1}{8} \sum_{\lambda_a,\lambda_b,\lambda_1,\lambda_2} \left(\mathcal{M}^{\sigma_3\sigma_4}_{\lambda_a\lambda_b\to\lambda_1\lambda_2\rho\rho}\right)^* \mathcal{M}^{\rho_3\rho_4}_{\lambda_a\lambda_b\to\lambda_1\lambda_2\rho\rho}\, g_{\sigma_3\rho_3}\, g_{\sigma_4\rho_4}\,. \end{aligned} \tag{2.21}$$

So far we have treated the exchanged mesonic object for $\rho^0\rho^0$ production as spin-1 particle. However, we should take into account the fact that the exchanged intermediate object is not a simple meson but may correspond to a whole family of daughter exchanges, that is, the reggeization of the intermediate ρ meson is necessary. For related works, where this effect was included in practical calculations, see e.g. [15, 20]. The "reggeization" of the amplitude given in Eq. (2.17) is included here for $\sqrt{s_{34}} \geqslant 2m_\rho$, only approximately, by replacing the ρ propagator both in the $\hat{t}$- and $\hat{u}$-channel amplitudes by

$$\Delta^{(\rho)}_{\rho_1\rho_2}(p) \to \Delta^{(\rho)}_{\rho_1\rho_2}(p) \left(\frac{s_{34}}{s_0}\right)^{\alpha_\rho(p^2)-1}\,, \tag{2.22}$$

where we take $s_0 = 4m_\rho^2$ and $\alpha_\rho(p^2) = 0.5 + 0.9\,t$ with the momentum transfer $t = p^2$.

To give the full physical amplitudes we should add absorptive corrections to the Born amplitudes (2.9) and (2.17) for the $pp \to pp\sigma\sigma$ and $pp \to pp\rho\rho$ reactions, respectively. For the details how to include the pp-rescattering corrections in the eikonal approximation for the four-body reaction see Sect. 3.3 of [17].

III. PRELIMINARY RESULTS

In this section we wish to present first results for the $pp \to pp\sigma\sigma$ and $pp \to pp\rho\rho$ processes corresponding to the diagrams shown in Fig. 1.

We start from a discussion of the $\pi^+\pi^-\pi^+\pi^-$ invariant mass distribution. In Fig. 2 we compare the $\sigma\sigma$- and $\rho\rho$-contributions to the CERN-ISR data [21] at $\sqrt{s} = 62$ GeV. Here, the four pions are restricted to lie in the rapidity region $|y_\pi| < 1.5$ and the cut [2] $|x_p| > 0.9$ is imposed on the outgoing protons. In Ref. [21] five contributions to the four-pion spectrum were identified. A 4π phase-space term with total angular momentum $J = 0$, two $\rho\pi\pi$ terms with $J = 0$ and $J = 2$, and two $\rho\rho$ terms with $J = 0$ and $J = 2$. In the following we will compare the 4π phase-space term with our $\sigma\sigma$ result, the $\rho\rho$ terms with our $\rho\rho$ result. The theoretical results correspond to the calculation including absorptive corrections related to the pp nonperturbative interaction in the initial and final state. The ratio of full and Born cross sections $\langle S^2 \rangle$ (the gap survival factor) is approximately $\langle S^2 \rangle = 0.4$. In our calculation both the $\mathbb{P}\mathbb{P}$ and the $\mathbb{P}f_{2\mathbb{R}}$, $f_{2\mathbb{R}}\mathbb{P}$, $f_{2\mathbb{R}}f_{2\mathbb{R}}$ exchanges were included. At the ISR energy the $f_{2\mathbb{R}}$ exchanges, including their interference terms with the $\mathbb{P}\mathbb{P}$ one, give about 50% to the total cross section.

In the left panel of Fig. 2 we compare our $\sigma\sigma$ contribution assuming the coupling constants (2.12) with the 4π ($J = 0$, phase space) ISR data (marked as full data points). We present results for two different forms of off-shell meson form factor, the exponential type (2.13), $\Lambda_{off,E} = 1.6$ GeV, and the monopole type (2.14), $\Lambda_{off,Mp} = 1.6$ GeV, see the black lower line and the red upper line, respectively. There is quite a good agreement between our $\sigma\sigma$ result with a monopole form factor and the 4π ($J = 0$, phase space) data. Note that this implies that the set B of $\mathbb{P}\sigma\sigma$ and $f_{2\mathbb{R}}\sigma\sigma$ couplings, which are larger than the corresponding pion couplings, seems to be preferred.

In the right panel of Fig. 2 we compare our result for the $\rho\rho$ contribution to corresponding ISR data [3]. In the calculation of the $\rho\rho$ contribution we take into account the intermediate ρ meson reggeization. The reggeization leads to an extra strong damping of the large $M_{4\pi}$ cross section. The effect of reggeization is expected only when the separation in rapidity between the two produced resonances is large. We will return to this issue in the further part of this section. We note that our model is able to give a qualitative account of the ISR $\rho\rho$ data for $M_{4\pi} \gtrsim 1.4$ GeV within the large experimental errors.

The total 4π experimental data (marked as open data points in the left panel of Fig. 2) are also shown for comparison. In Ref. [21] an integrated (total) cross section of 46 μb at $\sqrt{s} = 62$ GeV was estimated. There are other processes besides the ones of (2.1) contributing to the 4π final state, such as resonance production shown in the diagrams in Fig. 6 of Appendix A. Thus, the $\sigma\sigma$ and the $\rho\rho$ contributions considered here should not be expected to fit the ISR data precisely. In addition, the ISR 4π data includes also a large $\rho^0\pi^+\pi^-$ ($J = 0$ and $J = 2$) component (see Figs. 3b and 3d of [21]) with an enhancement in the $J = 2$ term which was interpreted there as a $f_2(1720)$ state. Also the $\rho^0\rho^0$ ($J = 2$) term indicates a signal of $f_2(1270)$ state; see Fig. 3e of [21]. Therefore, a consistent model for the resonance and continuum contributions, including the interference effects between them, would be required to better describe the ISR data. We leave this interesting problem for future studies.

[2] The Feynman-x variable was defined as $x_p = 2p_{z,p}/\sqrt{s}$ in the center-of-mass frame with $p_{z,p}$ the longitudinal momentum of the outgoing proton.

[3] Here we plotted the sum of the experimental cross section $\sigma = \sigma_{J=0} + \sigma_{J=2}$ for the $J = 0$ and $J = 2$ $\rho\rho$ terms (see Figs. 3c and 3e in [21], respectively) and the corresponding error is approximated as $\delta\sigma = \sqrt{\delta^2_{J=0} + \delta^2_{J=2}}$.

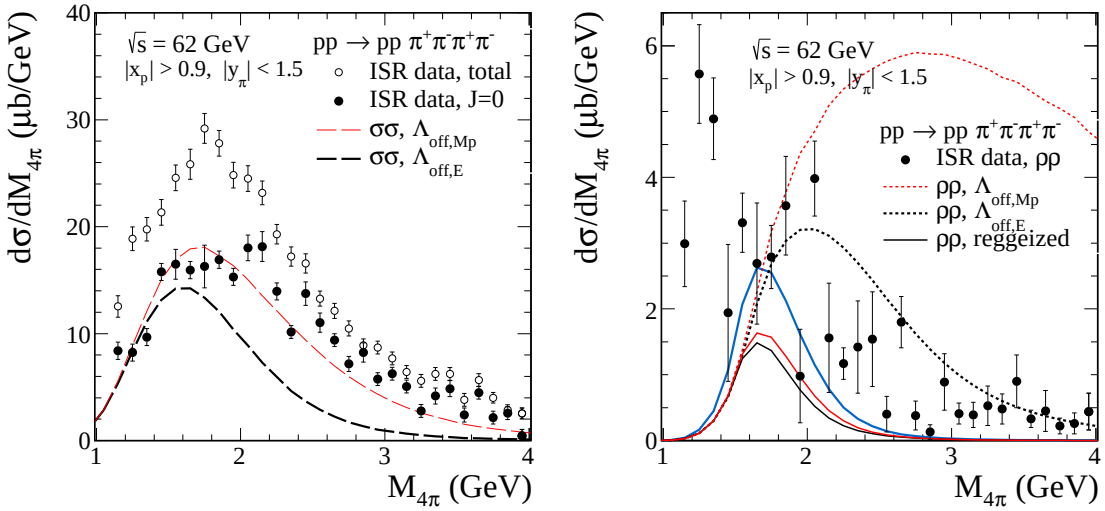

FIG. 2: Invariant mass distributions for the central $\pi^+\pi^-\pi^+\pi^-$ system compared to the CERN-ISR data [21] at $\sqrt{s} = 62$ GeV. In the left panel the lines represent results for the $\sigma\sigma$ contribution only and with the enhanced pomeron/reggeon-σ-σ couplings (2.12). We used two forms of the off-shell meson form factor, the exponential form (2.13) with $\Lambda_{off,E} = 1.6$ GeV (the black lines) and the monopole form (2.14) with $\Lambda_{off,Mp} = 1.6$ GeV (the red thin lines). In the right panel the lines represent results for the $\rho\rho$ contribution without (the dotted lines) and with (the solid lines) the inclusion of the intermediate ρ meson reggeization. For comparison, the upper blue solid line was obtained with the monopole form factor and $\Lambda_{off,Mp} = 1.8$ GeV. The absorption effects were included here.

In Fig. 3 we show our preliminary four-pion invariant mass distributions for experimental cuts relevant for the RHIC and LHC experiments. In the calculation of the $\sigma\sigma$ and the $\rho\rho$ contributions the pomeron and $f_{2\mathbb{R}}$ exchanges were included. Imposing limitations on pion (pseudo)rapidities, e.g. $|\eta_\pi| < 1$, and going to higher energies strongly reduces the role of subleading $f_{2\mathbb{R}}$ exchanges. The gap survival factors $\langle S^2 \rangle$ estimated within the eikonal approximation are 0.30, 0.21, 0.23 for $\sqrt{s}$ = 0.2, 7, 13 TeV, respectively. In the case of $\sigma\sigma$ contribution we use two sets of the coupling constants; standard (2.11) and enhanced ones (2.12).

The correlation in rapidity of pion pairs (Y_3, Y_4) (e.g., Y_3 means $Y_{\pi^+\pi^-}$ where the pions are produced from a meson decay) for both the $\sigma\sigma$ and the $\rho\rho$ contributions is displayed in Fig. 4 for $\sqrt{s} = 200$ GeV. For the $\sigma\sigma$ contribution, see the top panel, we observe a strong correlation $Y_3 \approx Y_4$. For the $\rho\rho$ case the (Y_3, Y_4) distribution extends over a much broader range of $Y_3 \neq Y_4$ which is due to the exchange of the spin-1 particle. However, as discussed in the section devoted to the formalism we may include, at least approximately, the effect of reggeization of the intermediate ρ meson. In the left and right bottom panels we show the results without and with the ρ meson reggeization, respectively. As shown in the right panel this effect becomes crucial when the separation in rapidity between the two ρ mesons increases. After the reggeization is performed the two-dimensional distribution looks very similar as for the $\sigma\sigma$ case. The reggeization effect discussed here is also closely related to the damping of the four-pion invariant mass distribution discussed already in Fig. 2.

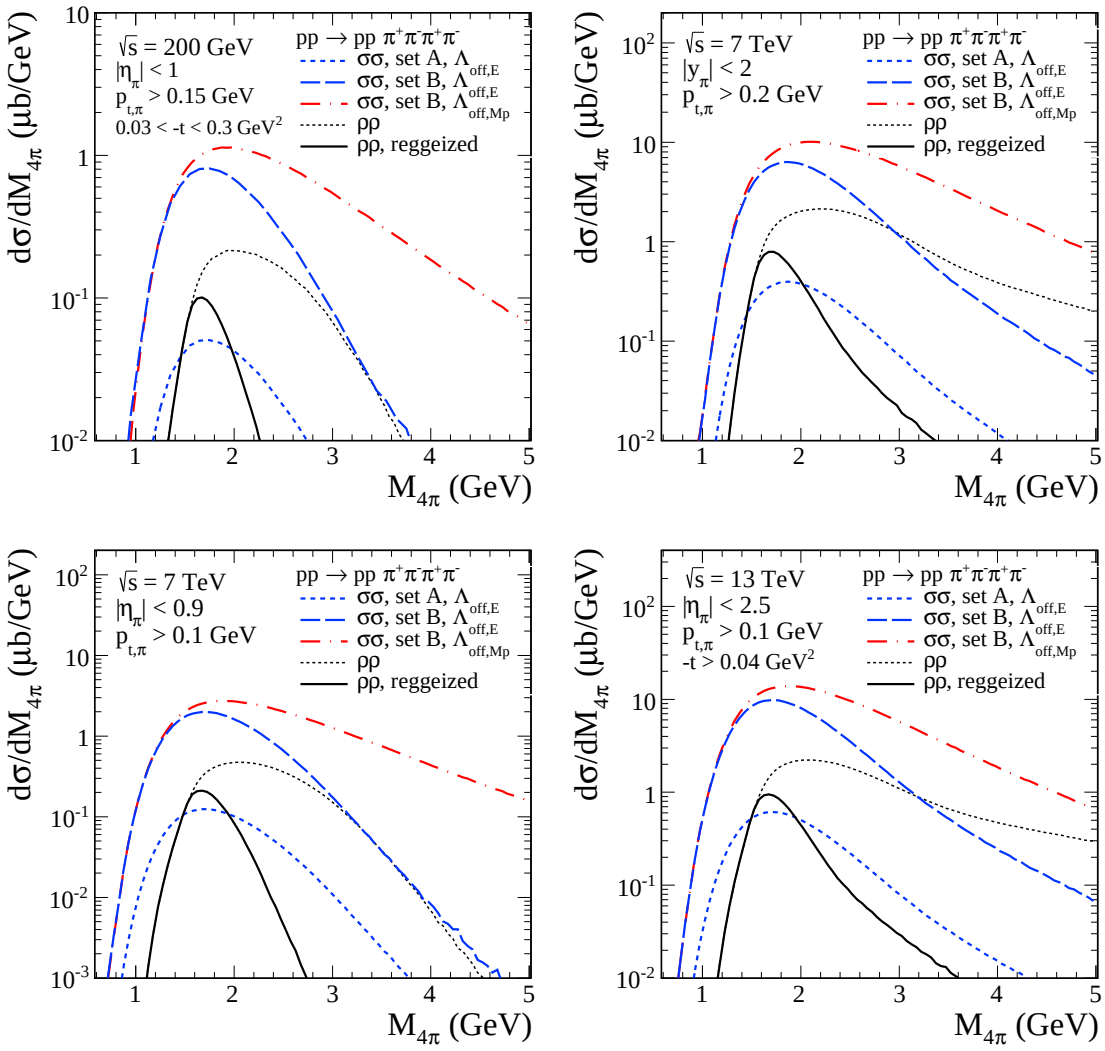

FIG. 3: Four-pion invariant mass distributions for different center-of-mass energies $\sqrt{s}$ and experimental kinematical cuts. The black lines represent results for the $\rho\rho$ contribution, the blue lines for the $\sigma\sigma$ contribution. The exponential off-shell meson form factors (2.13) with $\Lambda_{off,E} = 1.6$ GeV were used. For the case of $\sigma\sigma$ contribution only the red dot-dashed line was obtained with the monopole form factor and $\Lambda_{off,Mp} = 1.6$ GeV. The absorption effects were included here.

In Table I we have collected integrated cross sections in μb with different experimental cuts for the exclusive $\pi^+\pi^-\pi^+\pi^-$ production including only the contributions shown in Fig. 1. The collected results were obtained in the calculations with the tensor pomeron and reggeon exchanges. In the calculations the off-shell-meson form factor (2.13) with $\Lambda_{off,E} = 1.6$ GeV was used. No absorption effects were included in the quoted numbers. The full cross section can be obtained by multiplying the Born cross section by the corresponding gap survival factor $\langle S^2 \rangle$. These factors depend on the kinematic cuts and are 0.40 (ISR), 0.46 (STAR, lower $|t|$), 0.30 (STAR, higher $|t|$), 0.21 ($\sqrt{s}$ = 7 TeV), 0.19 ($\sqrt{s}$ = 13 TeV), 0.23 ($\sqrt{s}$ = 13 TeV, with cuts on $|t|$). The cross sections for the $\rho\rho$ final state found here are more than three orders of magnitude larger than the cross sections for the $\gamma\gamma \to \rho\rho$ and double scattering mechanisms considered recently in [18].

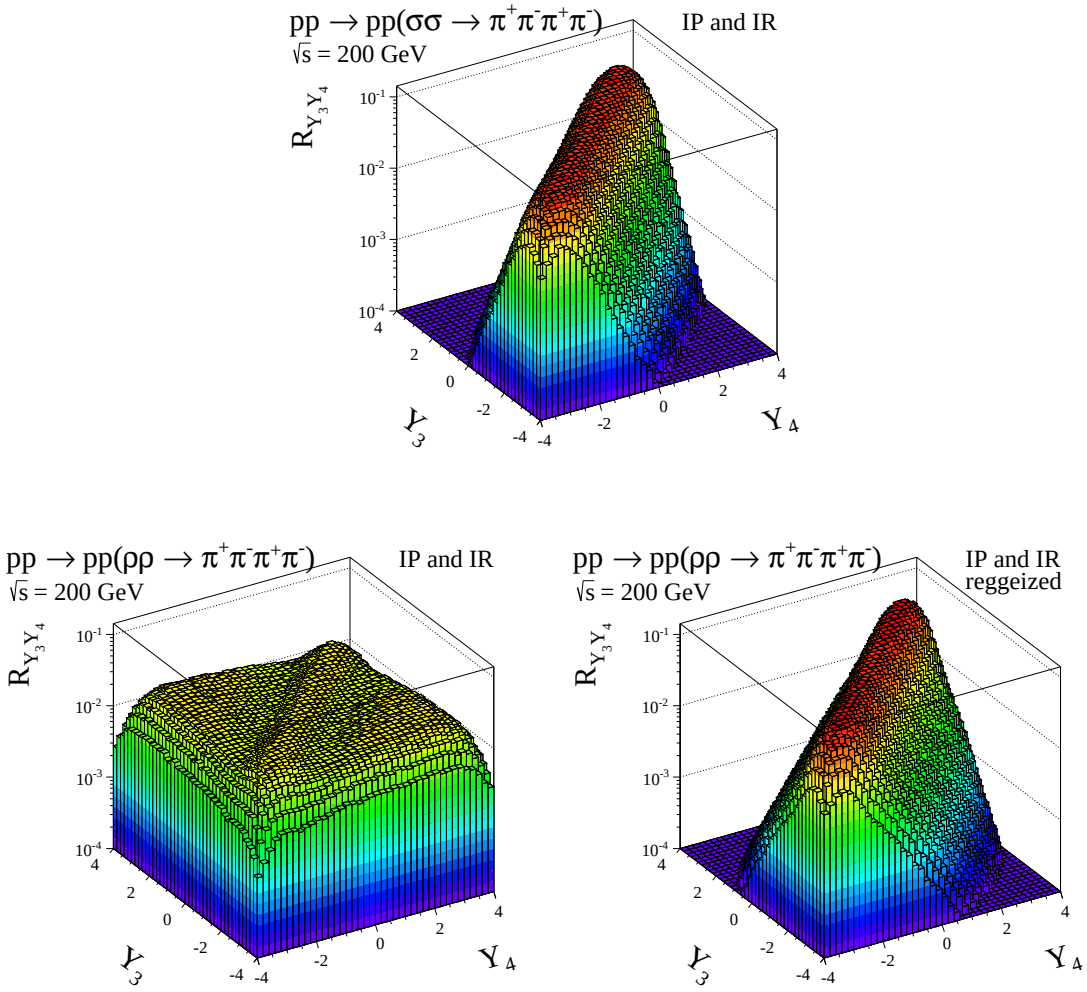

FIG. 4: The distributions in (Y_3, Y_4) space for the reaction $pp \to pp\pi^+\pi^-\pi^+\pi^-$ via fusion of two tensor pomerons and $f_{2\mathbb{R}}$ reggeons at $\sqrt{s} = 200$ GeV. Plotted is the ratio $R_{Y_3Y_4} = \frac{d^2\sigma}{dY_3 dY_4} / \int dY_3 dY_4 \frac{d^2\sigma}{dY_3 dY_4}$. We show the $\sigma\sigma$ contribution (top panel) and the $\rho\rho$ contribution (bottom panels) without (left panel) and with (right panel) the ρ meson reggeization included. Here $\Lambda_{off,E} = 1.6$ GeV was used.

Finally, in Fig. 5, we discuss some observables which are very sensitive to the absorptive corrections. Quite a different pattern can be seen for the Born case and for the case with absorption included. The absorptive corrections lead to significant modification of the shape of the ϕ_{pp} distribution (ϕ_{pp} is the azimuthal angle between the p_t vectors of the outgoing protons) and lead to an increase of the cross section for the proton four-momentum transfer $t = t_1 = t_2$ at large $|t|$. This effect could be verified in future experiments when both protons are measured which should be possible for ATLAS-ALFA [5] and CMS-TOTEM.

TABLE I: The integrated "Born level" (no gap survival factors) cross sections in μb for the central exclusive $\pi^+\pi^-\pi^+\pi^-$ production in pp collisions via the $\sigma\sigma$ and $\rho\rho$ mechanisms given in Fig. 1 for some typical experimental cuts. The $\sigma\sigma$ contribution was calculated using the coupling constants (2.12) while the $\rho\rho$ contribution without and with (in the parentheses) the inclusion of the intermediate ρ meson reggeization.

		Cross sections in μb	
$\sqrt{s}$, TeV	Cuts	$\sigma\sigma$	$\rho\rho$
0.062	$\lvert y_\pi\rvert < 1.5$, $\lvert x_p\rvert > 0.9$	37.92	10.66 (2.17)
0.2	$\lvert\eta_\pi\rvert < 1$, $p_{t,\pi} > 0.15$ GeV, $0.005 < -t < 0.03$ GeV^2	0.30	0.10 (0.02)
0.2	$\lvert\eta_\pi\rvert < 1$, $p_{t,\pi} > 0.15$ GeV, $0.03 < -t < 0.3$ GeV^2	2.94	0.88 (0.17)
7	$\lvert\eta_\pi\rvert < 0.9$, $p_{t,\pi} > 0.1$ GeV	10.40	2.79 (0.53)
7	$\lvert y_\pi\rvert < 2$, $p_{t,\pi} > 0.2$ GeV	34.88	17.94 (2.20)
13	$\lvert\eta_\pi\rvert < 1$, $p_{t,\pi} > 0.1$ GeV	16.18	3.56 (0.72)
13	$\lvert\eta_\pi\rvert < 2.5$, $p_{t,\pi} > 0.1$ GeV	120.06	45.58 (6.21)
13	$\lvert\eta_\pi\rvert < 2.5$, $p_{t,\pi} > 0.1$ GeV, $-t > 0.04$ GeV^2	47.52	18.08 (2.44)

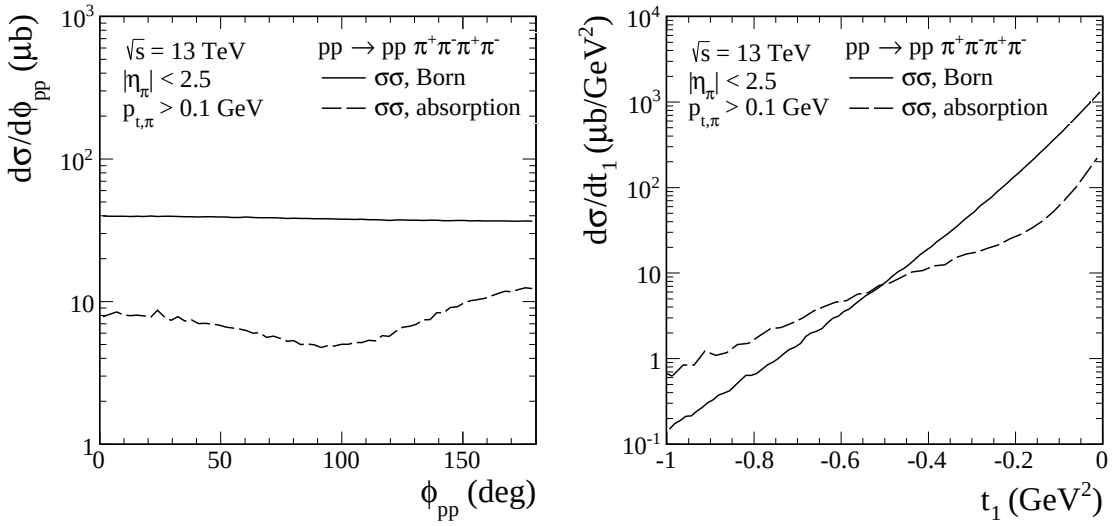

FIG. 5: Distributions in proton-proton relative azimuthal angle (the left panel) and in four-momentum squared of one of the protons (the right panel) for the central $\sigma\sigma \to \pi^+\pi^-\pi^+\pi^-$ contribution at $\sqrt{s} = 13$ TeV with the kinematical cuts specified in the legend. The solid line corresponds to the Born calculations and the long-dashed line corresponds to the result including the pp absorptive corrections. Here the enhanced pomeron/reggeon-σ-σ couplings (2.12) and the exponential form of off-shell meson form factor (2.13) with $\Lambda_{off,E} = 1.6$ GeV were used.

IV. CONCLUSIONS

In the present paper we have presented first estimates of the contributions with the intermediate $f_0(500)f_0(500)$, $\rho(770)\rho(770)$ resonance pairs to the reaction $pp \to pp\pi^+\pi^-\pi^+\pi^-$ which is being analyzed experimentally by the STAR, ALICE, CMS, and ATLAS Collaborations. The results were obtained within a model where the pomeron and $f_{2\mathbb{R}}$ reggeon are treated as effective tensor exchanges. The results for processes with

the exchange of heavy (compared to pion) mesons strongly depend on the details of the hadronic form factors. By comparing the theoretical results and the cross sections found in the CERN-ISR experiment [21] we fixed the parameters of the off-shell meson form factor and the $\mathbb{P}\sigma\sigma$ and $f_{2\mathbb{R}}\sigma\sigma$ couplings. The corresponding values of parameters can be verified by future experimental results obtained at RHIC and LHC.

We have made estimates of the integrated cross sections for different experimental situations as well as shown several differential distributions. The pion-pair rapidities of the two σ mesons are strongly correlated ($Y_3 \approx Y_4$). This is due to a strong interference effect between the $\hat{t}$- and $\hat{u}$-channel amplitudes. For the $\rho\rho$ contribution the situation is the following. If we take for the propagator of the exchanged ρ in Fig. 1, right panel, the standard particle propagator the $Y_3 - Y_4$ correlation is very weak. But for a reggeized ρ propagator we get again a strong $Y_3 - Y_4$ correlation, similar to that found in the $\sigma\sigma$ case; see Fig. 4. This is understandable since the reggeization suppresses contributions where the two produced ρ mesons have large subsystem energies, i.e. where there is a large rapidity distance between the two ρ mesons.

We have found in this paper that the diffractive mechanism in proton-proton collisions considered by us leads to the cross section for the $\rho\rho$ final state more than three orders of magnitude larger than the corresponding cross section for $\gamma\gamma \to \rho\rho$ and double scattering photon-pomeron (pomeron-photon) mechanisms considered recently in [18].

Closely related to the reaction $pp \to pp\pi^+\pi^-\pi^+\pi^-$ studied by us here is the 4π production in ultra-peripheral nucleus-nucleus collisions. A phenomenological study of the reaction mechanism of $AA \to AA\rho^0\rho^0$ was performed in Ref. [19]. The application of our methods, based on the tensor-pomeron concept, to collisions involving nuclei is an interesting problem which goes, however, beyond the scope of the present work.

To summarize: we have given a consistent treatment of the $\pi^+\pi^-\pi^+\pi^-$ production via two scalar σ mesons and two vector ρ mesons in an effective field-theoretic approach. A measurable cross section of order of a few μb was obtained for the $pp \to pp\pi^+\pi^-\pi^+\pi^-$ process which should give experimentalists interesting challenges to check and explore it.

Appendix A: Four-pion production through $f_0 \to \sigma\sigma$ and $f_0 \to \rho\rho$ mechanisms

Here we discuss the diffractive production of the scalar $f_0(1370)$, $f_0(1500)$, and $f_0(1710)$ resonances decaying at least potentially into the $\pi^+\pi^-\pi^+\pi^-$ final state. We present relevant formulas for the resonance contributions that could be used in future analyses. At present a precise calculation of the resonance contributions to the four-pion channel is not possible as some details of the relevant decays are not well understood.

The production and decay properties of the scalar mesons in the 4π channel, such as the $f_0(1370)$ and $f_0(1500)$ states, have been investigated extensively in central diffractive production by the WA102 Collaboration at $\sqrt{s} = 29.1$ GeV [22–24] and in $p\bar{p}$ and $\bar{p}n$ annihilations by the Crystal Barrel Collaboration [25]. In central production, see Fig. 3 of [23], there is a very clear signal from $f_0(1500)$ in the 4π spectra, especially in the $\sigma\sigma$ channel, and some evidence of the broad $f_0(1370)$ resonance in the $\rho\rho$ channel. In Fig. 1 of Ref. [24] the $J^{PC} = 0^{++}$ $\rho\rho$ wave from the $\pi^+\pi^-\pi^+\pi^-$ channel in four different ϕ_{pp} intervals (each of 45^o) was shown. A peak below $M_{4\pi} \simeq 1500$ MeV was clearly seen which can be interpreted as the interference effect of the $f_0(1370)$ state, the $f_0(1500)$ state and the broad 4π background. In principle, also the contributions from the $f_0(1710)$ and

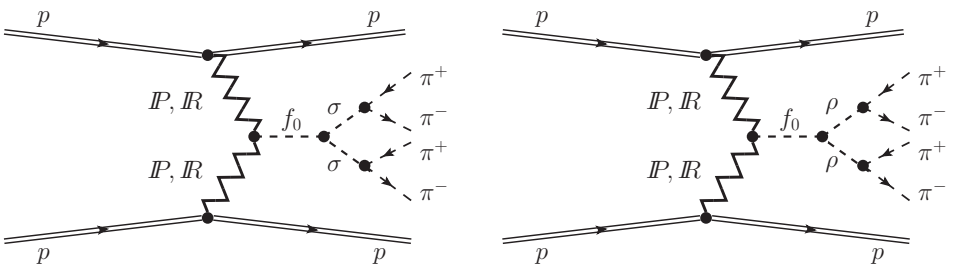

FIG. 6: The "Born level" diagrams for double-pomeron/reggeon central exclusive production of $\pi^+\pi^-\pi^+\pi^-$ through $f_0 \to \sigma\sigma$ (left diagram) and $f_0 \to \rho\rho$ (right diagram) in proton-proton collisions.

$f_0(2020)$ are not excluded. In Table 1 of [24] the percentage of each resonance in three intervals of the so-called "glueball filter variable" (dP_T) was shown. The idea being that for small differences in the transverse momentum vectors between the two exchanged "particles" an enhancement in the production of glueballs relative to $q\bar{q}$ states may occur. The dP_T dependence and the ϕ_{pp} distributions presented there are similar to what was found in the analysis of the $\pi^+\pi^-$ channel [26]. In Refs. [27, 28] it was shown that also the $f_0(1710)$ state has a similar behaviour in the azimuthal angle ϕ_{pp} and in the dP_T variable as the $f_0(1500)$ state. That is, all the undisputed $q\bar{q}$ states are observed to be suppressed at small dP_T, but the glueball candidates $f_0(1500)$, $f_0(1710)$, together with the enigmatic $f_0(980)$, survive. It was shown in [24] that the $f_0(1370)$ and $f_0(2000)$ have similar dP_T and ϕ_{pp} dependences. The fact that $f_0(1370)$ and $f_0(1500)$ states have different dP_T and ϕ_{pp} dependences confirms that these are not simply J dependent phenomena [4]. This is also true for the $J = 2$ states, where the $f_2(1950)$ state has different dependences compared to the $f_2(1270)$ and $f_2'(1520)$ states [26]. We wish to emphasize that in [15] we obtained a good description of the WA102 experimental distributions [26, 32, 33] for the scalar and pseudoscalar mesons within the framework of the tensor pomeron approach. The dP_T and ϕ_{pp} effects can be understood as being due to the fact that in general more than one pomeron-pomeron-meson coupling structure is possible [15]. The behaviour of the tensor $f_2(1270)$ state was discussed recently in [7]; see Figs. 4 and 5 there.

In the following we present our analytic expressions for the diagrams of Fig. 6 for $I\!P I\!P$ fusion only. The extension to include also $I\!P f_{2I\!R}$, $f_{2I\!R} I\!P$ and $f_{2I\!R} f_{2I\!R}$ fusion is straightforward.

a. $pp \to pp(f_0 \to \sigma\sigma)$

Here we consider the amplitude for the reaction (2.4) through an s-channel scalar resonance $f_0 \to \sigma\sigma$; see Fig. 6 (left diagram). Here f_0 stands, for one of the $f_0(1370)$, $f_0(1500)$, $f_0(1710)$ states.

[4] Some essential discrepancy for $f_0(1370)$ and $f_0(1500)$ states in the different decay channels was discussed, e.g., in Refs. [29, 30]. In Ref. [31], by using a three-flavor chiral effective approach, the authors found that $f_0(1710)$ is predominantly the gluonic state and the $\rho\rho \to 4\pi$ decay channel is strongly suppressed.

In the high-energy small-angle approximation we can write this amplitude as

$$\begin{aligned}\mathcal{M}^{(f_0\to\sigma\sigma)}_{\lambda_a\lambda_b\to\lambda_1\lambda_2\sigma\sigma} &\simeq 3\beta_{\mathbb{P}NN}\,2(p_1+p_a)_{\mu_1}(p_1+p_a)_{\nu_1}\,\delta_{\lambda_1\lambda_a}\,F_1(t_1)\,\frac{1}{4s_1}(-is_1\alpha'_{\mathbb{P}})^{\alpha_{\mathbb{P}}(t_1)-1}\\ &\times\Gamma^{(\mathbb{P}\mathbb{P}f_0)\,\mu_1\nu_1,\mu_2\nu_2}(q_1,q_2)\,\Delta^{(f_0)}(p_{34})\,\Gamma^{(f_0\sigma\sigma)}(p_3,p_4)\\ &\times\frac{1}{4s_2}(-is_2\alpha'_{\mathbb{P}})^{\alpha_{\mathbb{P}}(t_2)-1}\,3\beta_{\mathbb{P}NN}\,2(p_2+p_b)_{\mu_2}(p_2+p_b)_{\nu_2}\,\delta_{\lambda_2\lambda_b}\,F_1(t_2)\,,\end{aligned}\tag{A1}$$

where $s_1=(p_1+p_3+p_4)^2$, $s_2=(p_2+p_3+p_4)^2$, $q_1=p_a-p_1$, $q_2=p_b-p_2$, $t_1=q_1^2$, $t_2=q_2^2$, and $p_{34}=p_3+p_4$.

The effective Lagrangians and the vertices for $\mathbb{P}\mathbb{P}$ fusion into an f_0 meson are discussed in Appendix A of [15]. As was shown there the tensorial $\mathbb{P}\mathbb{P}f_0$ vertex corresponds to the sum of two lowest values of (l,S), that is $(l,S)=(0,0)$ and $(2,2)$ with coupling parameters $g'_{\mathbb{P}\mathbb{P}M}$ and $g''_{\mathbb{P}\mathbb{P}M}$, respectively. The vertex, including a form factor, reads then as follows ($p_{34}=q_1+q_2$)

$$i\Gamma^{(\mathbb{P}\mathbb{P}f_0)}_{\mu\nu,\kappa\lambda}(q_1,q_2)=\left(i\Gamma'^{(\mathbb{P}\mathbb{P}f_0)}_{\mu\nu,\kappa\lambda}\mid_{bare}+i\Gamma''^{(\mathbb{P}\mathbb{P}f_0)}_{\mu\nu,\kappa\lambda}(q_1,q_2)\mid_{bare}\right)\tilde{F}^{(\mathbb{P}\mathbb{P}f_0)}(q_1^2,q_2^2,p_{34}^2)\,;\tag{A2}$$

see (A.21) of [15]. Unfortunately, the pomeron-pomeron-meson form factor is not well known as it is due to nonperturbative effects related to the internal structure of the respective meson. In practical calculations we take the factorized form for the $\mathbb{P}\mathbb{P}f_0$ form factor

$$\tilde{F}^{(\mathbb{P}\mathbb{P}f_0)}(q_1^2,q_2^2,p_{34}^2)=F_M(q_1^2)F_M(q_2^2)F^{(\mathbb{P}\mathbb{P}f_0)}(p_{34}^2)\tag{A3}$$

normalised to $\tilde{F}^{(\mathbb{P}\mathbb{P}f_0)}(0,0,m_{f_0}^2)=1$. We will further set

$$F^{(\mathbb{P}\mathbb{P}f_0)}(p_{34}^2)=\exp\left(\frac{-(p_{34}^2-m_{f_0}^2)^2}{\Lambda_{f_0}^4}\right),\quad \Lambda_{f_0}=1\text{ GeV}\,.\tag{A4}$$

For the $f_0\sigma\sigma$ vertex we have

$$i\Gamma^{(f_0\sigma\sigma)}(p_3,p_4)=ig_{f_0\sigma\sigma}M_0\,F^{(f_0\sigma\sigma)}(p_{34}^2)\,,\tag{A5}$$

where $g_{f_0\sigma\sigma}$ is an unknown parameter. We assume $g_{f_0\sigma\sigma}>0$ and $F^{(f_0\sigma\sigma)}(p_{34}^2)=F^{(\mathbb{P}\mathbb{P}f_0)}(p_{34}^2)$; see Eq. (A4).

b. $pp\to pp(f_0\to\rho\rho)$

Now we consider the amplitude for the reaction (2.15) through f_0 exchange in the s-channel as shown in Fig. 6 (right diagram). In the high-energy approximation we can write the amplitude as shown in (2.16) with

$$\begin{aligned}\mathcal{M}^{(f_0\to\rho\rho)\,\rho_3\rho_4}_{\lambda_a\lambda_b\to\lambda_1\lambda_2\rho\rho} &\simeq 3\beta_{\mathbb{P}NN}\,2(p_1+p_a)_{\mu_1}(p_1+p_a)_{\nu_1}\,\delta_{\lambda_1\lambda_a}\,F_1(t_1)\,\frac{1}{4s_1}(-is_1\alpha'_{\mathbb{P}})^{\alpha_{\mathbb{P}}(t_1)-1}\\ &\times\Gamma^{(\mathbb{P}\mathbb{P}f_0)\,\mu_1\nu_1,\mu_2\nu_2}(q_1,q_2)\,\Delta^{(f_0)}(p_{34})\,\Gamma^{(f_0\rho\rho)\,\rho_3\rho_4}(p_3,p_4)\\ &\times\frac{1}{4s_2}(-is_2\alpha'_{\mathbb{P}})^{\alpha_{\mathbb{P}}(t_2)-1}\,3\beta_{\mathbb{P}NN}\,2(p_2+p_b)_{\mu_2}(p_2+p_b)_{\nu_2}\,\delta_{\lambda_2\lambda_b}\,F_1(t_2)\,,\end{aligned}\tag{A6}$$

where we take for the $f_0\rho\rho$ vertex the following ansatz

$$\begin{aligned}
&\Gamma^{(f_0\rho\rho)\,\rho_3\rho_4}(p_3,p_4) = \\
&g'_{f_0\rho\rho}\,\frac{2}{M_0^3}\left[p_3^2 p_4^2 g^{\rho_3\rho_4} - p_4^2 p_3^{\rho_3} p_3^{\rho_4} - p_3^2 p_4^{\rho_3} p_4^{\rho_4} + (p_3\cdot p_4)\, p_3^{\rho_3} p_4^{\rho_4}\right] F'^{(f_0\rho\rho)}(p_3^2,p_4^2,p_{34}^2) \\
&+ g''_{f_0\rho\rho}\,\frac{2}{M_0}\left[p_4^{\rho_3} p_3^{\rho_4} - (p_3\cdot p_4) g^{\rho_3\rho_4}\right] F''^{(f_0\rho\rho)}(p_3^2,p_4^2,p_{34}^2)
\end{aligned} \tag{A7}$$

with $g'_{f_0\rho\rho}$ and $g''_{f_0\rho\rho}$ being free parameters. Different form factors F' and F'' are allowed a priori. The vertex in Eq. (A7) fulfils the following relations:

$$p_{3\,\rho_3}\Gamma^{(f_0\rho\rho)\rho_3\rho_4}(p_3,p_4) = 0\,, \qquad p_{4\,\rho_4}\Gamma^{(f_0\rho\rho)\rho_3\rho_4}(p_3,p_4) = 0\,. \tag{A8}$$

Once evidence for one or more of the f_0 resonances discussed here is obtained from RHIC and/or LHC experiments the formulae given in this appendix should be useful. Then, it will hopefully be possible to determine empirically the coupling parameters of the relevant vertices: $\mathbb{P}\mathbb{P}f_0$, $f_0\sigma\sigma$ and $f_0\rho\rho$.

Acknowledgments

We are indebted to Leszek Adamczyk, Lidia Görlich, Radosław Kycia, Wolfgang Schäfer and Jacek Turnau for useful discussions. This research was partially supported by the MNiSW Grant No. IP2014 025173 (Iuventus Plus), the Polish National Science Centre Grant No. DEC-2014/15/B/ST2/02528 (OPUS) and by the Centre for Innovation and Transfer of Natural Sciences and Engineering Knowledge in Rzeszów.

---

[1] L. Adamczyk, W. Guryn, and J. Turnau, *Central exclusive production at RHIC,* Int.J.Mod.Phys. **A29** no. 28, (2014) 1446010, arXiv:1410.5752 [hep-ex].

[2] T. A. Aaltonen *et al.*, (CDF Collaboration), *Measurement of central exclusive $\pi^+\pi^-$ production in $p\bar{p}$ collisions at $\sqrt{s} = 0.9$ and 1.96 TeV at CDF,* Phys. Rev. **D91** (2015) 091101, arXiv:1502.01391 [hep-ex].

[3] M. Albrow, J. Lewis, M. Żurek, A. Święch, D. Lontkovskyi, I. Makarenko, and J. S. Wilson. The public note called *Measurement of Central Exclusive Hadron Pair Production in CDF* is available at `http://www-cdf.fnal.gov/physics/new/qcd/GXG_14/webpage/`.

[4] R. Schicker, *Diffractive production of mesons,* EPJ Web Conf. **81** (2014) 01005, arXiv:1410.6060 [hep-ph].

[5] R. Staszewski, P. Lebiedowicz, M. Trzebiński, J. Chwastowski, and A. Szczurek, *Exclusive $\pi^+\pi^-$ Production at the LHC with Forward Proton Tagging,* Acta Phys.Polon. **B42** (2011) 1861–1870, arXiv:1104.3568 [hep-ex].

[6] (CMS Collaboration), *Measurement of exclusive $\pi^+\pi^-$ production in proton-proton collisions at $\sqrt{s} = 7$ TeV,* CMS-PAS-FSQ-12-004.

[7] P. Lebiedowicz, O. Nachtmann, and A. Szczurek, *Central exclusive diffractive production of the $\pi^+\pi^-$ continuum, scalar and tensor resonances in pp and $p\bar{p}$ scattering within the tensor Pomeron approach,* Phys. Rev. **D93** (2016) 054015, arXiv:1601.04537 [hep-ph].

[8] P. Lebiedowicz and A. Szczurek, *Exclusive $pp \to pp\pi^+\pi^-$ reaction: From the threshold to LHC,* Phys.Rev. **D81** (2010) 036003, arXiv:0912.0190 [hep-ph].

[9] P. Lebiedowicz, R. Pasechnik, and A. Szczurek, *Measurement of exclusive production of scalar χ_{c0} meson in proton-(anti)proton collisions via $\chi_{c0} \to \pi^+\pi^-$ decay,* Phys.Lett. **B701** (2011) 434–444, arXiv:1103.5642 [hep-ph].

[10] P. Lebiedowicz and A. Szczurek, *$pp \to ppK^+K^-$ reaction at high energies,* Phys.Rev. **D85** (2012) 014026, arXiv:1110.4787 [hep-ph].

[11] P. Lebiedowicz and A. Szczurek, *Exclusive $pp \to nn\pi^+\pi^+$ reaction at LHC and RHIC,* Phys.Rev. **D83** (2011) 076002, arXiv:1005.2309 [hep-ph].

[12] P. Lebiedowicz and A. Szczurek, *Revised model of absorption corrections for the $pp \to pp\pi^+\pi^-$ process,* Phys. Rev. **D92** (2015) 054001, arXiv:1504.07560 [hep-ph].

[13] O. Nachtmann, *Considerations concerning diffraction scattering in quantum chromodynamics,* Annals Phys. **209** (1991) 436–478.

[14] C. Ewerz, M. Maniatis, and O. Nachtmann, *A Model for Soft High-Energy Scattering: Tensor Pomeron and Vector Odderon,* Annals Phys. **342** (2014) 31–77, arXiv:1309.3478 [hep-ph].

[15] P. Lebiedowicz, O. Nachtmann, and A. Szczurek, *Exclusive central diffractive production of scalar and pseudoscalar mesons; tensorial vs. vectorial pomeron,* Annals Phys. **344** (2014) 301–339, arXiv:1309.3913 [hep-ph].

[16] A. Bolz, C. Ewerz, M. Maniatis, O. Nachtmann, M. Sauter, and A. Schöning, *Photoproduction of $\pi^+\pi^-$ pairs in a model with tensor-pomeron and vector-odderon exchange,* JHEP **1501** (2015) 151, arXiv:1409.8483 [hep-ph].

[17] P. Lebiedowicz, O. Nachtmann, and A. Szczurek, *ρ^0 and Drell-Söding contributions to central exclusive production of $\pi^+\pi^-$ pairs in proton-proton collisions at high energies,* Phys. Rev. **D91** (2015) 074023, arXiv:1412.3677 [hep-ph].

[18] V. P. Goncalves, B. D. Moreira, and F. S. Navarra, *Double vector meson production in photon - hadron interactions at hadronic colliders,* arXiv:1605.05840 [hep-ph].

[19] M. Kłusek-Gawenda and A. Szczurek, *Double-scattering mechanism in the exclusive $AA \to AA\rho^0\rho^0$ reaction in ultrarelativistic collisions,* Phys. Rev. **C89** (2014) 024912, arXiv:1309.2463 [nucl-th].

[20] A. Cisek, P. Lebiedowicz, W. Schäfer, and A. Szczurek, *Exclusive production of ω meson in proton-proton collisions at high energies,* Phys.Rev. **D83** (2011) 114004, arXiv:1101.4874 [hep-ph].

[21] A. Breakstone *et al.*, (ABCDHW Collaboration), *Evidence for $f_2(1720)$ production in the reaction pomeron-pomeron $\to \pi^+\pi^-\pi^+\pi^-$,* Z. Phys. **C58** (1993) 251–256.

[22] D. Barberis *et al.*, (WA102 Collaboration), *A study of the centrally produced $\pi^+\pi^-\pi^+\pi^-$ channel in pp interactions at 450 GeV/c,* Phys. Lett. **B413** (1997) 217–224, arXiv:9707021 [hep-ex].

[23] D. Barberis *et al.*, (WA102 Collaboration), *A Spin analysis of the 4π channels produced in central pp interactions at 450-GeV/c,* Phys.Lett. **B471** (2000) 440–448, arXiv:9912005 [hep-ex].

[24] D. Barberis *et al.*, (WA102 Collaboration), *A study of the $f_0(1370)$, $f_0(1500)$, $f_0(2000)$ and $f_2(1950)$ observed in the centrally produced 4π final states,* Phys.Lett. **B474** (2000) 423–426, arXiv:0001017 [hep-ex].

[25] A. Abele *et al.*, (Crystal Barrel Collaboration), *Study of f_0 decays into four neutral pions,* Eur.Phys.J. **C19** (2001) 667–675.

[26] D. Barberis *et al.*, (WA102 Collaboration), *A coupled channel analysis of the centrally produced K^+K^- and $\pi^+\pi^-$ final states in pp interactions at 450 GeV/c,* Phys.Lett. **B462** (1999) 462–470,

arXiv:9907055 [hep-ex].

[27] A. Kirk, (WA102 Collaboration), *New effects observed in central production by experiment WA102 at the CERN Omega Spectrometer,* Nucl. Phys. **A663** (2000) 608–612, arXiv:hep-ph/9907302 [hep-ph].

[28] A. Kirk, *Resonance production in central pp collisions at the CERN Omega spectrometer,* Phys.Lett. **B489** (2000) 29–37, arXiv:0008053 [hep-ph].

[29] E. Klempt and A. Zaitsev, *Glueballs, Hybrids, Multiquarks. Experimental facts versus QCD inspired concepts,* Phys.Rept. **454** (2007) 1–202, arXiv:0708.4016 [hep-ph].

[30] W. Ochs, *The Status of Glueballs,* J.Phys. **G40** (2013) 043001, arXiv:1301.5183 [hep-ph].

[31] S. Janowski, F. Giacosa, and D. H. Rischke, *Is $f_0(1710)$ a glueball?,* Phys. Rev. **D90** (2014) 114005, arXiv:1408.4921 [hep-ph].

[32] D. Barberis *et al.*, (WA102 Collaboration), *A study of pseudoscalar states produced centrally in pp interactions at 450 GeV/c,* Phys.Lett. **B427** (1998) 398–402, arXiv:9803029 [hep-ex].

[33] D. Barberis *et al.*, (WA102 Collaboration), *Experimental evidence for a vector like behavior of Pomeron exchange,* Phys.Lett. **B467** (1999) 165–170, arXiv:9909013 [hep-ex].